


## Research Article

# Landscape evolution and ancient settlement patterns in a small river basin of the Huangshui River and the prehistoric Wangjinglou City, Central China

Yinan Liao<sup>a</sup> , Peng Lu<sup>b</sup>, Duowen Mo<sup>c</sup>, Qian Wu<sup>d</sup>, Xiangli Zhao<sup>d</sup>, Ye Li<sup>c</sup>, Panpan Chen<sup>b</sup> and Hui Wang<sup>a</sup>

<sup>a</sup>Key Laboratory of Archaeological Sciences and Cultural Heritage, Chinese Academy of Social Sciences (Chinese Academy of History & University of Chinese Academy of Social Sciences), Beijing 100710, China; <sup>b</sup>Institute of Geographical Sciences, Henan Academy of Sciences, Zhengzhou 450006, China; <sup>c</sup>Laboratory for Earth Surface Process, Ministry of Education, College of Urban and Environmental Sciences, Peking University, Beijing 100871, China and <sup>d</sup>Zhengzhou Institute of Cultural Relics and Archaeology, 450000 Zhengzhou, China

### Abstract

Prehistoric humans seem to have preferred inhabiting small river basins, which were closer in distance to most settlements compared to larger rivers. The Holocene landscape evolution is considered to have played a pivotal role in shaping the spatiotemporal patterns of these settlements. In this study, we conducted comprehensive research on the relationship between landscape evolution and settlement distribution within the Huangshui River basin, which is a representative small river in Central China with numerous early settlements, including a prehistoric city known as the Wangjinglou site (WJL). Using geoarchaeological investigations, optically stimulated luminescence dating, pollen analysis, and grain-size analysis, we analyzed the characteristics of the Holocene environment. The results indicate the presence of two distinct geomorphic systems, namely the red clay hills and the river valley. The red clay hills, formed in the Neogene, represent remnants of the Songshan piedmont alluvial fan that was eroded by rivers. There are three grades of terraces within the river valley. T3 is a strath terrace and formed around 8.0 ka. Both T2 and T1 are fill terraces, which were developed around 4.0 ka and during the historical period, respectively. The sedimentary features and pollen analysis indicate the existence of an ancient lake-swamp on the platform during 11.0–9.0 ka. This waterbody gradually shrank during 9.0–8.0 ka, and ultimately disappeared after 8.0 ka. Since then, the development of large-scale areas of water ceased on the higher geomorphic units. River floods also cannot reach the top of these high geomorphic units, where numerous prehistoric settlements are located, including the Xia–Shang cities of the WJL site. Our research demonstrates that landscape stability supported the long-term and sustainable development of ancient cultures and facilitated the establishment of the WJL ancient cities in the region.

**Keywords:** Small river basin, prehistoric settlement, ancient city, landscape evolution, human–environment interaction, Central China

### INTRODUCTION

The origin and development of human civilization has always been intricately intertwined with the presence and influence of rivers (Macklin et al., 2015). This connection is particularly evident during prehistoric times, with numerous renowned river basins around the world being adorned with ancient settlements. The Yellow River, the Yangtze River, the Indus River, the Ganges River, the Mekong River, the Euphrates River, the Tigris River, and the Mississippi River are all noted as rivers of ancient civilizations (Kidder et al., 2005; Wang et al., 2018; Zhang et al., 2022).

Although sites of prehistoric cultural importance are expressed throughout the entire river basin of large rivers, there is an important phenomenon that deserves attention and consideration. In comparison to the main watercourse of a large river, it can be observed that most prehistoric settlements are located in tributary

basins (Lu et al., 2022a). Firstly, most prehistoric settlements are closer to tributaries than to the main watercourse of a large river. In China, limited evidence of Neolithic–Bronze Age settlements is observed along the main channels of large rivers such as the Yangtze, Yellow, and Huai rivers. However, some tributaries, such as the Yiluo River, the Jing River, the Hang River, and the Shuangji River are dotted with densely distributed prehistoric settlements (National Cultural Heritage Administration, 1991, 1999, 2003). Secondly, the most significant sites that have contributed to the origin and development of civilization are situated on tributaries of large rivers. For example, the Liangzhu Site is adjacent to the Tiaoxi River (Liu et al., 2017), the Shimao Site is situated near the Tuwei River (Sun et al., 2018), the Erlitou Site is found along the Yiluo River (Xu et al., 2004), the Taosi Site is adjacent to the Fen River (He, 2018), and the Shijiahe Site is situated near the Tianmen River (Liu et al., 2017). Therefore, the small river basin seems to possess great ancient cultural and ecological significance.

The significant historical and ecological values of small river basins are closely related to the characteristics and evolution of regional landscapes. During prehistoric periods, settlement

**Corresponding author:** Peng Lu; Email: [bulate\\_0@163.com](mailto:bulate_0@163.com)

**Cite this article:** Liao Y, Lu P, Mo D, Wu Q, Zhao X, Li Y, Chen P, Wang H (2025). Landscape evolution and ancient settlement patterns in a small river basin of the Huangshui River and the prehistoric Wangjinglou City, Central China. *Quaternary Research* 1–11. <https://doi.org/10.1017/qua.2024.45>



locations were meticulously selected based on careful consideration of the natural landscape (Shimada *et al.*, 1991; Garcia *et al.*, 1999; Tinner *et al.*, 2000; Lü *et al.*, 2019; Chen *et al.*, 2021; Wilson *et al.*, 2022). The establishment and development of human settlements has been profoundly influenced by the characteristics of relevant natural factors, such as landform, hydrology, and vegetation (Zhou *et al.*, 2005; Dong *et al.*, 2006; Liu *et al.*, 2010; Lu *et al.*, 2012; Xu *et al.*, 2015; Liao *et al.*, 2019; Ren *et al.*, 2021). Therefore, there is a strong correlation between the spatiotemporal distribution of prehistoric settlements and early landscape features. Investigation of the landscape evolution provides a valuable avenue for exploring the mechanisms underlying the dense distribution of prehistoric settlements, as well as the emergence and decline of regional cultures within small river basins.

This study focuses on a representative small basin of the Huangshui River in Central China, which is home to numerous prehistoric settlements, including significant ancient cities of the Wangjinglou (WJL) site. Using geoarchaeological investigations, optically stimulated luminescence (OSL) dating, pollen analysis, and grain-size analysis, we conducted a comprehensive study of the environmental characteristics and landscape evolution within the basin. Our findings are of great significance in elucidating the mechanisms that underlie the dense distribution of prehistoric settlements within the small river basin, thereby contributing to a deeper understanding of regional landscape evolution and human–environment interactions.

## REGIONAL SETTING

The Huangshui River, a tertiary tributary of the Huai River, originates in the eastern foothills of Songshan Mountain. It meanders southeastwards, eventually joining the Shuangji River within the plains area before merging into the Huai River (Fig. 1). The Huangshui River is a typical small river, with a length of merely 30 km and a basin area spanning 110 km<sup>2</sup>. The river basin lies within the transitional zone between the Chinese Loess Plateau and the North China Plain, characterized by a flat topography, loess deposits, and a relatively dense distribution of deep gullies. The region has a continental monsoon climate, with a mean annual temperature of 15.2°C and an average annual precipitation of 600 mm. The prevailing vegetation consists of broadleaved deciduous forests and shrubs (Wang *et al.*, 1989).

Despite the small size of the river, there are numerous prehistoric settlement sites within the Huangshui River basin. Archaeological investigations have revealed more than 50 prehistoric settlements (9.0–3.0 ka) distributed in the basin, resulting in a remarkable settlement density of 0.46 per km<sup>2</sup> (National Cultural Heritage Administration, 1991). These settlements belong to different archaeological cultures, including the Peiligang period (9.0–7.0 ka), Yangshao period (7.0–5.0 ka), Longshan period (5.0–4.0 ka), and Xia–Shang periods (4.0–3.0 ka) (Lu *et al.*, 2016). Many settlements are significant in the origin of Chinese civilization, including a prominent prehistoric city known as the WJL site (Wu *et al.*, 2011; Gu *et al.*, 2012).

The WJL site is located in the middle reaches of the Huangshui River, at the geographic coordinates 113°43′08.48″E, 34°26′53.35″N, at an altitude of 119 m. The site area is approximately 120,000 m<sup>2</sup>, with a length of 300 m and a width of 400 m (Wu *et al.*, 2011). The site dates back to the Xia–Shang periods, mainly associated with the Erlitou culture (3.7–3.5 ka) and Erligang culture (3.6–3.3 ka). Many valuable remains and relics, including bronzes,

jades, pottery, stone tools, mussels, roads, large rammed earth foundations, sacrificial pits, houses, stoves, pottery kilns, ash pits, wells, and tombs have been unearthed at the site (Wu *et al.*, 2011; Wu, 2022). Notably, two prehistoric city sites dating back to the Erlitou culture and Erligang culture have been unearthed at this site, indicating the important position of the WJL site during the Xia–Shang periods (Wu *et al.*, 2011; Gu *et al.*, 2012). As a high-grade city settlement of the Erlitou and Erligang cultures, the WJL site played a key role in the complex system of capitals and cities during the early stages of civilization (Gu *et al.*, 2012; Zhang, 2012; Chen *et al.*, 2018; Feng, 2019).

## MATERIALS AND METHODS

### *Field survey and stratigraphic characteristics*

Since 2020, we have conducted a comprehensive geoarchaeological investigation in the WJL site region and the Huangshui River basin. During the survey process, we meticulously examined a significant number of stratigraphic sections in the region. Most sections were measured, recorded, and mapped in terms of distinct sedimentary layers. The regional sedimentary characteristics, distribution, and ages were also analyzed and inferred in the field.

Based on our geoarchaeological investigation, the exposed strata in the region can be traced back to the Neogene period. Near the WJL site, a section known as WAC (113°43′06.95″E, 34°27′04.92″N) exhibits a substantial Neogene red clay layer that is exposed for approximately 2 m without a base (Fig. 2). This layer is commonly found in the region, typically containing white calcium deposits and gravels, which are likely indicative of fluvial deposition. Another Neogene stratum, characterized by the presence of red clay and abundant gravels, is visible in a section along the west bank of the Huangshui River (HWB, 113°42′53.20″E, 34°27′09.10″N). Owing to lack of deposition or erosion, the strata from the Early to Middle Pleistocene are absent in the region. The Neogene red clay layer is directly overlain by a widely distributed Late Pleistocene aeolian loess, namely the Malan loess, with an average thickness of approximately 5 m.

The regional Holocene strata, which are generally located on the Late Pleistocene loess, can be broadly classified into two distinct types. The first is aeolian loess, predominantly observed in elevated regions. The second type consists of alluvial deposits that include both fluvial and lacustrine sediments, primarily located in the lower areas near the river. To provide comprehensive stratigraphic descriptions, we present illustrative examples from three distinct sections: the WJL section, the Madong (MD) section, and the Zhoujiawan (ZJW) section.

### *The WJL section*

The section is situated in the northeastern part of the WJL site, at 113°43′53.69″E and 34°27′2.87″N, at an elevation of 135 m. The exposed strata of this section, which extends to a depth of 200 cm, can be clearly divided into two units:

Layer 1, which is approximately 30 cm in thickness, consists of a deposit of Holocene loess.

Layer 2 represents an aeolian sand stratum that is visibly exposed at an approximate depth of 170 cm. The sediment displays a uniform sorting and exceptionally pure composition, suggesting aeolian deposition rather than fluvial activity. The prevalent aeolian sand in the area is commonly believed to be wind transported from the nearby Yellow River (Lu *et al.*, 2019).

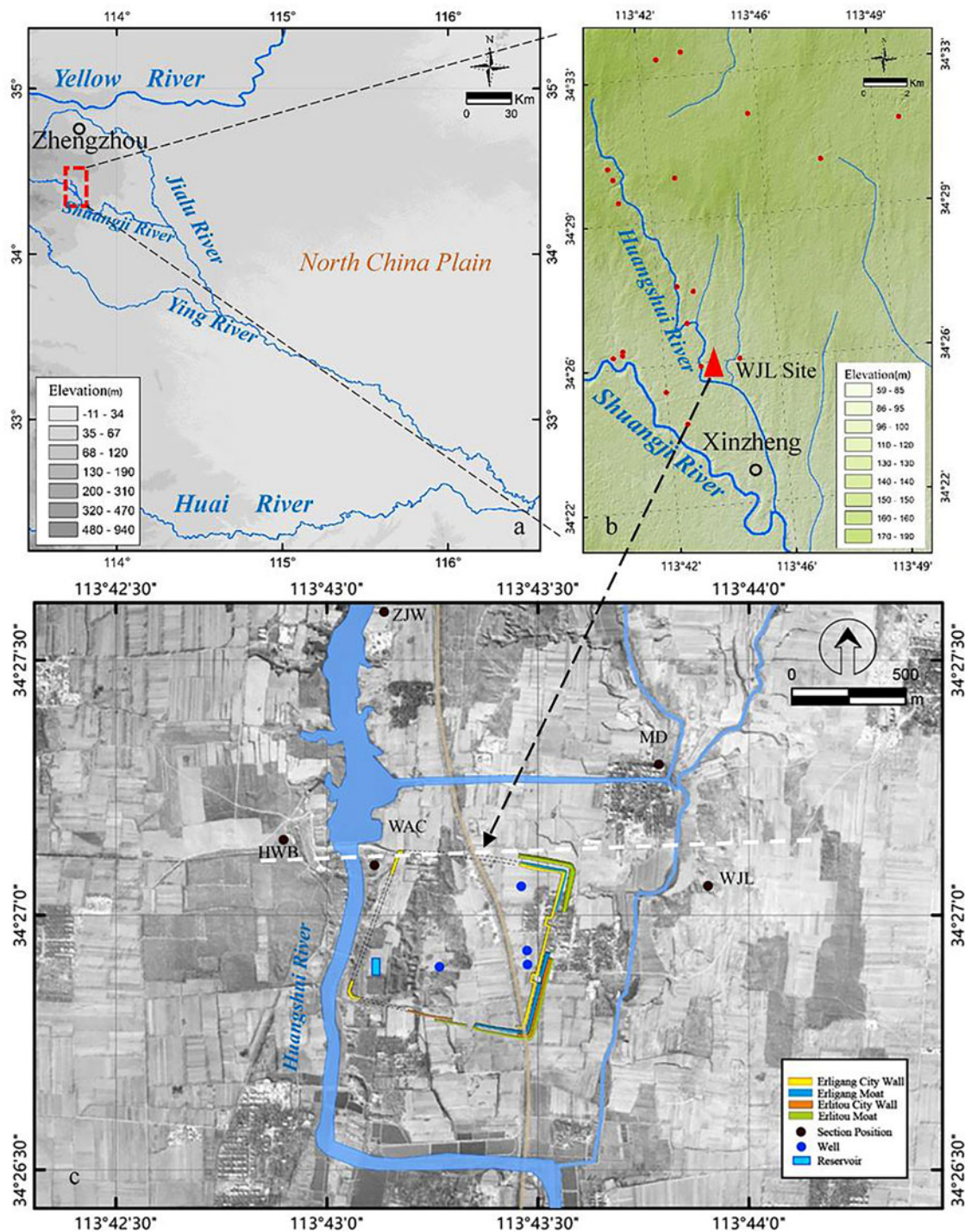


**Figure 1.** Research region: (a) Location of the Huangshui River basin. (b) Prehistoric sites in the Huangshui River basin. (c) The Wangjinglou (WJL) ancient city and research profiles. The white line indicates the location of the cross section in Figure 4.

#### The MD section

The MD section is located northeast of the WJL site, at  $34^{\circ}27'17.43''\text{N}$  and  $113^{\circ}43'47.15''\text{E}$ , at an elevation of 126 m. The exposed section reveals fluvial and lacustrine deposits, indicating the presence of extensive ancient lakes and swamps in the area. These alluvial sediments can extend eastwards to the eastern bank of a tributary of the Huangshui River. The MD section exhibits a total exposure of 300 cm and can be divided into three distinct units:

Layer 1 has an approximate thickness of 100 cm and is classified as color 7.5YR5-3 according to the Munsell Soil Color Book. The layer identified as loess exhibits a limited presence of ceramic pieces. Layer 2 consists of fluvial and lacustrine deposits, with a thickness of 185 cm. This layer displays a distinct horizontal bedding pattern and has a color of 7.5YR3-2 according to the Munsell Soil Color Book. Layer 3 consists of loess, which is exposed for a thickness of approximately 15 cm. The layer contains a higher

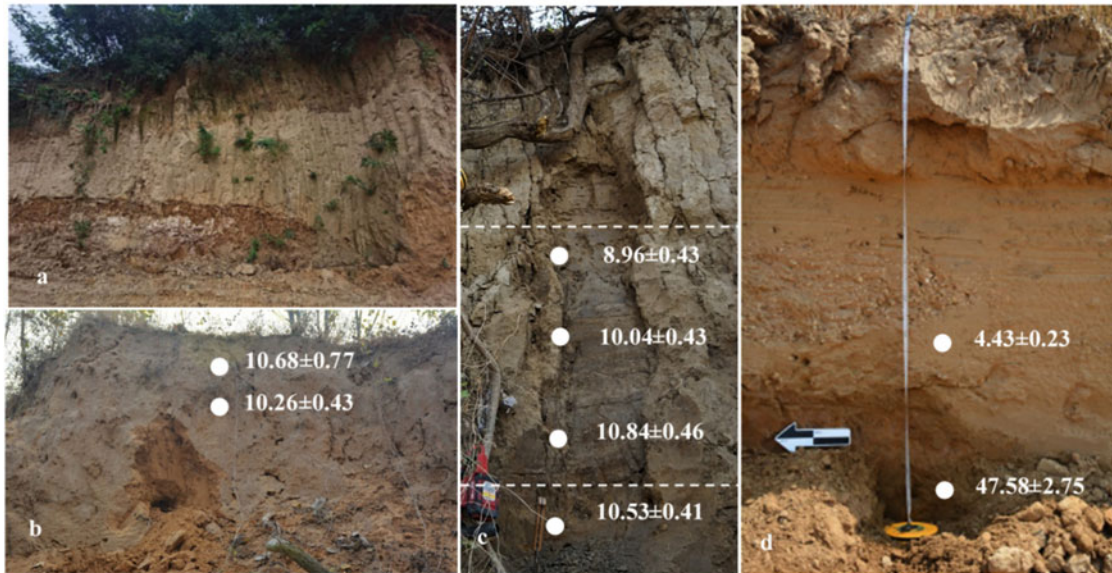


**Figure 2.** The geologic sections near the WJL site: (a) WAC; (b) Wangjinglou (WJL); (c) Madong (MD); (d) Zhoujiawan (ZJW). Ages are in ka.

concentration of rust spots compared to other layers, and its color is 7.5YR4-2 according to the Munsell Soil Color Book.

#### The ZJW section

The section is located on the east bank of the Huangshui River, at 34°28′32.07″N and 113°42′39.95″E, with an elevation of 114 m. The exposed section has a thickness of 150 cm and can be divided into three distinct units:

Layer 1 is Holocene secondary loess, which is about 60 cm thick and exhibits clear horizontal bedding. The layer contains a higher concentration of charcoal and has a color of 7.5YR5-3 according to the Munsell Soil Color Book.

Layer 2 is a sand and gravel layer with a thickness of 40 cm. This layer contains small-sized gravel, mostly with a diameter of less than 1 cm. The gravel exhibits excellent roundness and is observed as interbedded lenses sandwiched between two layers of sand. The color is 7.5YR5-2 according to the Munsell Soil Color Book.

Layer 3 consists of Late Pleistocene loess and is exposed to a depth of approximately 50 cm. The layer contains numerous rust spots and a higher concentration of charcoal, and the color is 7.5YR4-6 according to the Munsell Soil Color Book.

#### OSL dating

Eight OSL dating samples were collected, including four samples from the MD section, two samples from the ZJW section, and two samples from the WJL section. These samples were mainly collected from the alluvial deposits of each section for analyzing the process of fluvial geomorphic evolution within the basin. All samples were collected under light-tight conditions.

The OSL dating was performed according to the standard single-aliquot regenerative-dose (SAR) procedure at the Laboratory of Digital Environmental Archaeology, Institute of Geographical Sciences, Henan Academy of Sciences, China. Using sedimentation methods, the fine quartz particles (4–11 μm) were extracted after removing organic matter with 10% H<sub>2</sub>O<sub>2</sub> and dissolving carbonate

minerals with 10% HCl. The measuring device was a lexsys research instrument, which was manufactured in Germany. Uranium, thorium, and potassium contents of the samples were measured using neutron activation analysis (NAA). Age calculations incorporated in situ water contents measured in the field, with standard errors set at 5%. The aliquots obtained from measurements were used in the calculations (Zhang et al., 2009; Lai and Ou, 2013). The purity of quartz was then tested by infrared (IR) stimulation. All measurements were performed on a lexsys research luminescence reader. SAR protocols (Murray and Wintle, 2003) were used to determine the equivalent dose ( $D_e$ ) for fine-grained quartz. Fifteen aliquots were measured for each OSL sample. The dose rates and OSL ages were determined by the Dose Rate and Age Calculator ('DRAC') (Durcan et al., 2015).

#### Pollen analysis

Pollen samples were collected at 5 cm intervals from the fluvial and lacustrine sediments of the MD section. A total of 37 sediment samples were included in the pollen analysis at Jishou University. The samples were subjected to treatment with hydrochloric acid (HCl), sodium hydroxide (NaOH), hydrogen fluoride (HF), and acetolysis in order to eliminate impurities. *Lycopodium* spore tablets were added to determine pollen concentration. Pollen species identification primarily followed the Pollen Morphology of Chinese Plants (Wang et al., 1995). Subsequent statistical analyses and mapping were performed based on the specific identification results. The Tilia 1.7.16 software was used to construct pollen percentage diagrams.

#### Grain-size analysis

Grain-size samples were also collected from the MD section at intervals of 5 cm. Approximately 0.3 g of each sample were treated with a 30% H<sub>2</sub>O<sub>2</sub> solution to remove organic components, and then a 10% HCl solution was added to eliminate carbonates. Water was added to adjust the pH value, followed by the addition of (NaPO<sub>3</sub>)<sub>6</sub> before testing on the instrument. A Malvern 2000

laser particle size meter was used to measure grain sizes ranging from 0.01 to 2000  $\mu\text{m}$ . Grain-size parameters were calculated using the Folk–Ward method and classified according to international standards (Folk and Ward, 1957).

## RESULTS

### Chronology

The results of OSL dating are summarized in Table 1. The pre-heating test demonstrates that a preheating temperature of 220° C is suitable for fine-grained samples. The majority of samples exhibit an over-dispersion rate below 15%, which indicates a relatively concentrated distribution of effective dose. The recycling ratios fall within the range of 0.9 to 1.1, indicating successful correction for sensitivity changes. Recuperation is within an acceptable range of 5%. OSL decay curves demonstrate effective bleaching of the samples (Fig. 3).

In the WJL section, OSL dating samples were collected from both the upper and lower portions of the fine sand layer, denoted as HGS-02 and HGS-01, respectively. The age of HGS-02 was determined to be  $10.68 \pm 0.77$  ka, while HGS-01 yielded an age of  $10.26 \pm 0.43$  ka (Fig. 4).

Within the MD section, OSL dating samples were collected from the top, middle, and bottom of the lacustrine layer, as well as the top of the loess layer, designated as WJL-01, WJL-02, WJL-03, and WJL-04, respectively. Their ages were  $8.96 \pm 0.43$  ka,  $10.04 \pm 0.43$  ka,  $10.84 \pm 0.46$  ka, and  $10.53 \pm 0.41$  ka, respectively. Despite a slight inversion in WJL-03 and WJL-04, the dating results still fall within an acceptable margin of error.

The OSL samples of the ZJW section were collected from two different loess layers, which have been identified as ZJW-1 and ZJW-2. The age of ZJW-1 was determined to be  $4.43 \pm 0.23$  ka, while ZJW-2 yielded an age of  $47.58 \pm 2.75$  ka.

The new OSL ages are consistent with the overall dating results for the Shuangji River basin (Lu et al., 2022a), which also includes the Huangshui River. The dating results provide us with significant insights into the regional geomorphic patterns. Based on the dating results, terrain features, altitude, and material construction, these sections can be classified into three distinct geomorphic positions. The WJL section is situated on the highest geomorphic unit in the region, which is known as the red clay tableland. The WJL site is also located on this tableland. Both the MD and ZJW sections are located on the river terraces. However, the MD section is situated within the higher river terrace, whereas the ZJW section is positioned on the lower river terrace.

### Pollen assemblage

Owing to the low pollen content in the loess, we only conducted the pollen analysis on the lacustrine deposits of the MD section (Fig. 5). The results show that the regional vegetation was primarily characterized by terrestrial herbs, including *Artemisia*, *Aster*, *Taraxacum*, Chenopodiaceae, Gramineae, Cyperaceae, Leguminosae, *Humulus*, and others. Moisture-loving herbs, trees, and shrubs also played a significant role in the pollen results. Based on the recovered pollen assemblages and cluster analysis, three major vegetation zones were identified.

#### Zone 1 (285–200 cm)

The vegetation in this zone was predominantly composed of terrestrial herbs, such as *Artemisia*, *Aster*, *Taraxacum*, and

**Table 1.** Optically stimulated luminescence (OSL) dating results

Lab. no.	Sample no.	Depth (cm)	U (ppm)	Th (ppm)	K (%)	Rb (ppm)	Q-D <sub>e</sub> (Gy)	Aliquot no.	OD <sup>a</sup> (%)	w.c. <sup>b</sup> (%)	Q-dose rate	Q-age (ka)
L889	ZJW-01	55	2.08 ± 0.03	12.1 ± 0.07	1.68 ± 0.01	79.5 ± 0.95	16.89 ± 0.45	15	6.3 ± 0.5	4.30	3.82 ± 0.17	4.43 ± 0.23
L890	ZJW-02	115	2.32 ± 0.01	14.1 ± 0.18	1.65 ± 0.001	75.9 ± 1.13	180.97 ± 5.33	15	7.8 ± 1.3	7.60	3.78 ± 0.19	47.58 ± 2.75
L708	WJL-01	120	2.88 ± 0.10	8.95 ± 0.28	1.57 ± 0.01	71.6 ± 0.79	28.38 ± 0.22	15	3.0 ± 0.2	13.48	3.18 ± 0.15	8.96 ± 0.43
L709	WJL-02	200	2.13 ± 0.06	10.5 ± 0.21	1.74 ± 0.01	83.8 ± 1.68	32.14 ± 0.19	15	4.1 ± 0.4	14.94	3.20 ± 0.14	10.04 ± 0.43
L710	WJL-03	280	1.73 ± 0.03	10.6 ± 0.21	1.7 ± 0.01	82.2 ± 2.47	33.54 ± 0.32	15	3.3 ± 0.4	14.29	3.10 ± 0.13	10.84 ± 0.46
L711	WJL-04	300	1.51 ± 0.05	8.99 ± 0.26	1.63 ± 0.01	72.7 ± 2.18	32.94 ± 0.21	15	5.5 ± 0.5	7.98	3.13 ± 0.12	10.53 ± 0.41
L690	HGS-01	130	1.79 ± 0.03	8.35 ± 0.07	1.84 ± 0.01	78.6 ± 1.25	34.56 ± 0.64	15	4.0 ± 0.3	4.89	3.37 ± 0.13	10.26 ± 0.43
L707	HGS-02	50	1.80 ± 0.04	9.61 ± 0.16	1.6 ± 0.01	83.7 ± 0.91	36.35 ± 2.17	15	12.2 ± 1.8	4.20	3.40 ± 0.14	10.68 ± 0.77

<sup>a</sup>OD, over-dispersion.

<sup>b</sup>w.c., water content.

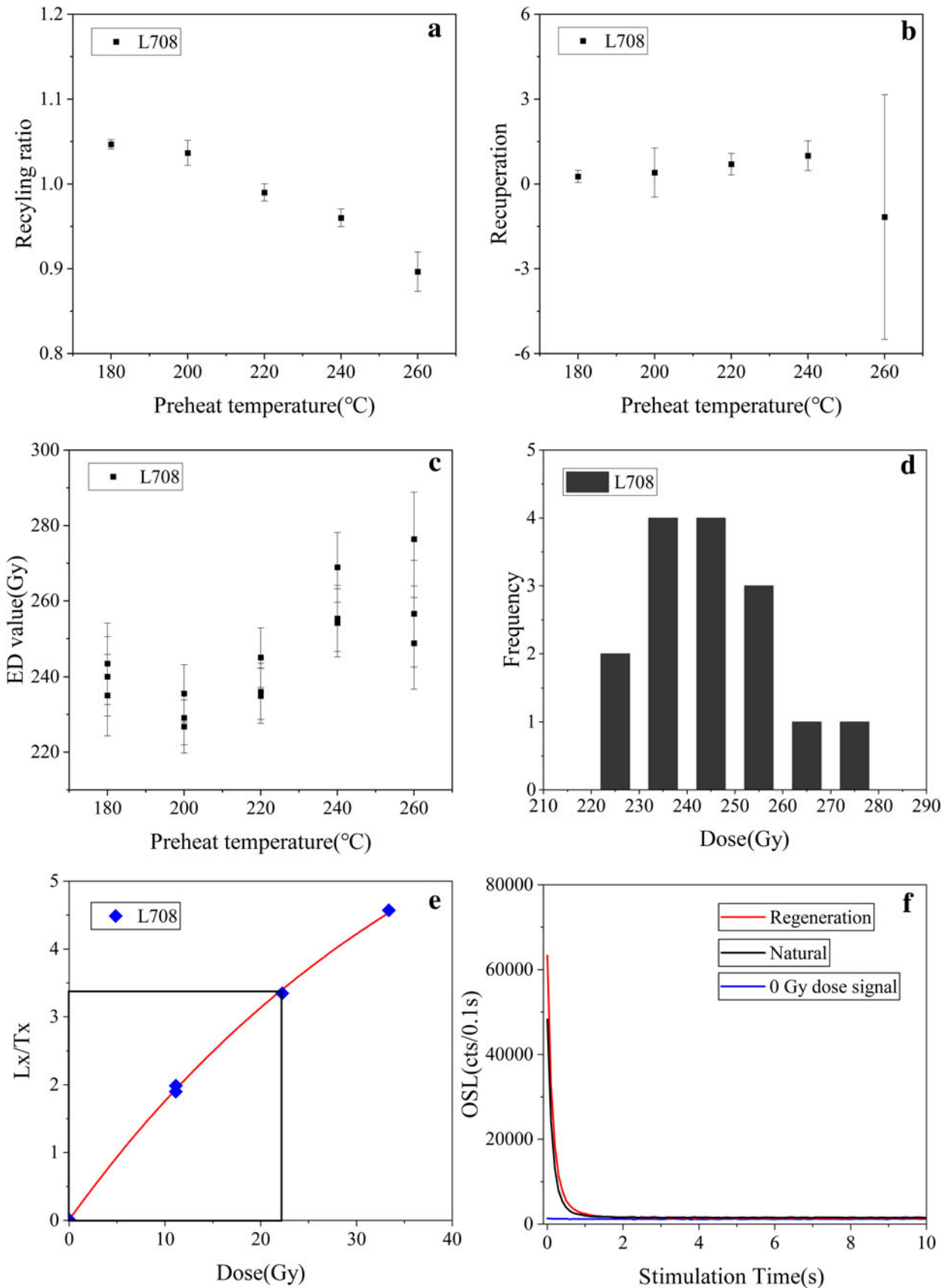


**Figure 3.** Graphs showing optically stimulated luminescence dating procedures: (a) recycling ratio; (b) recuperation; (c) preheating test; (d) recycling ratio histogram; (e) growth curve; (f) decay curves.

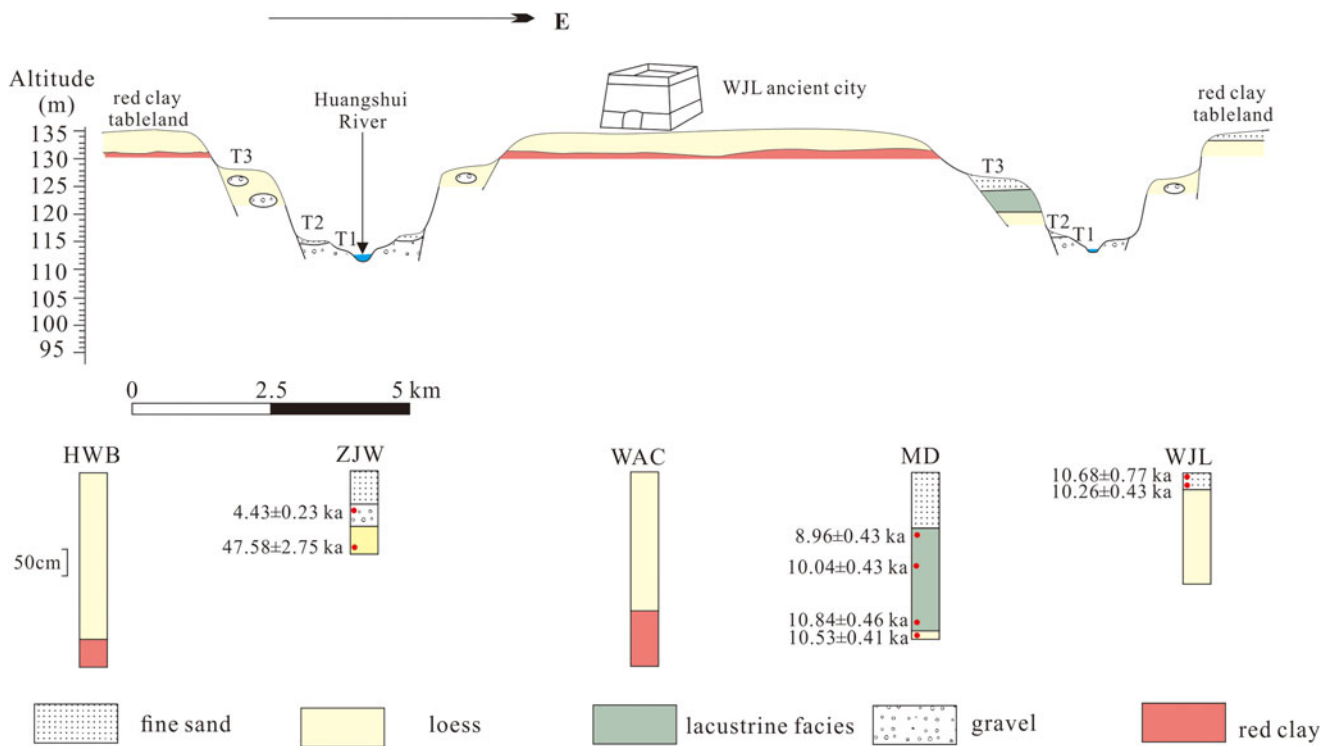


**Figure 4.** The regional cross section, indicated in Figure 1c, illustrates that the Wangjinglou (WJL) city site is situated on a Neogene red clay platform. The altitude indicates the elevation of the terrace surfaces. The stratigraphic scale has been marked alongside the ZJW section.

Chenopodiaceae, along with aquatic herbs like *Typha* and *Myriophyllum*. The zone revealed a reduced presence of arboreal and shrub species, including *Pinus*, *Quercus/deciduous*, *Alnus*, and *Ulmus*. The intermittent presence of ferns and algae, including *Selaginella* and *Zygnema*, was also observed. The prevailing feature of this era was the prevalence of herbaceous flora, with the presence of hygrophilous herbs indicating the existence of water in the area.

**Zone 2 (200–140 cm)**

The dominance of terrestrial herbs persisted in this zone, albeit with an augmented representation of hygrophilous herbs, arboreal species, and shrubs. Significantly, there was a notable increase in

the abundance of aquatic herbs, particularly *Typha*, which demonstrated an average six-fold augmentation during this stage. The results also reveal a marginal increase in the abundance of *Myriophyllum*. Moreover, there was an increasing trend observed in both the abundance and diversity of algae and fern species, which suggests a prevailing warm and humid ecological setting.

**Zone 3 (140–100 cm)**

This zone was characterized by an increasing presence of hygrophilous herbs, trees, and shrubs, including *Ulmus*, *Quercus/deciduous*, *Typha*, and *Myriophyllum*. However, terrestrial herbs continued to maintain their dominance and exhibited

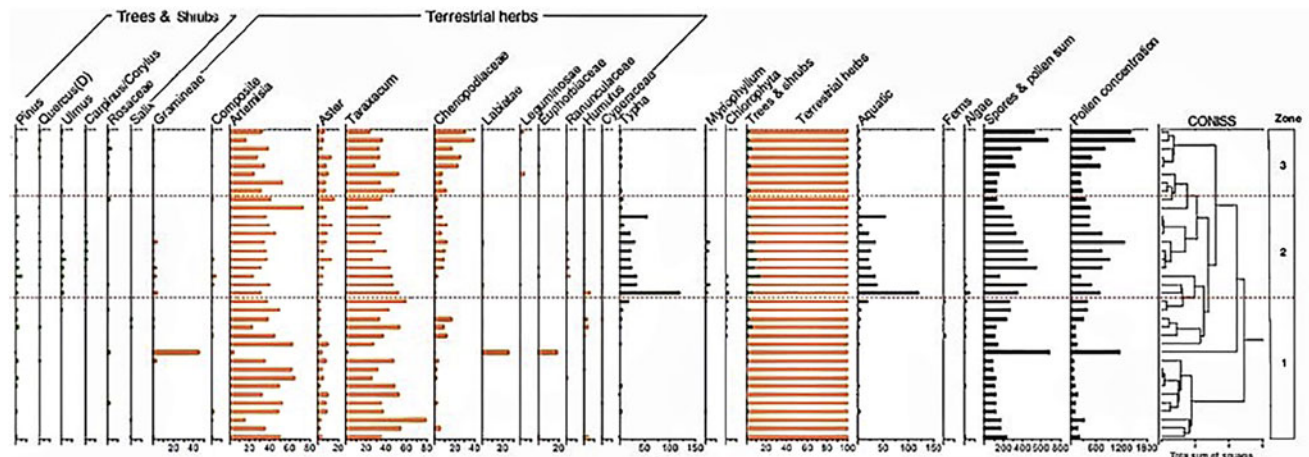


**Figure 5.** The pollen assemblage of the MD section indicates the presence of a stable lacustrine swamp landscape on Terrace T3 during the Early Holocene. After 8.0 ka, the ancient lake dried up due to river downcutting.

a persistent increase in abundance. The decline in diverse arboreal and hygrophilous herbaceous species, accompanied by an increase in xerophytic taxa such as Chenopodiaceae, implies a fluctuating arid environment.

The pollen assemblage of the MD section, which consistently aligns with the vegetation and landscape characteristics elucidated in previous regional pollen studies (Lu et al., 2022b), provides valuable insights into the genesis and demise of an ancient lake on the high terrace. According to our field survey and research on the fluvial landform evolution in the adjacent Shuangji River basin (Lu et al., 2019, 2022a), this would have been a small lake distributed along the river valley. The relatively concentrated age distribution suggests that the lake predominantly existed during the Early Holocene. The 8.0 ka age of lake extinction also serves as an indicator for the chronology of river downcutting and terrace formation. Since then, there has been no occurrence of large-scale water accumulation on the high terrace.

### Grain-size distribution

The grain-size results of the MD section are presented in Figure 6, illustrating three distinct types of particle distribution. These findings, which demonstrate a consistency with the results of numerous relevant studies in the region (Lu et al., 2019, 2022a), indicate variations in sedimentary environments and processes.

#### Stage 1 (285–200 cm)

The median size ranged from 32.48 to 22.18  $\mu\text{m}$ , with an average of 27.19  $\mu\text{m}$ , predominantly comprising silt. The sorting ranged from 1.700 to 1.892  $\phi$ , while the skewness varied between 0.366 and 0.427  $\phi$ , indicating a significantly positive skewness. The kurtosis values ranged from 1.157 to 1.270, indicating a distribution with a pronounced peak. The substantial median size and sand content of the sediments during this stage suggest a period characterized by diminished summer monsoon precipitation and weakened weathering, indicative of relatively colder climatic conditions. In conjunction with the stratigraphic and pollen data, it can be inferred that the dimensions of the ancient lakes and swamps during this period were relatively small, characterized by a limited water volume and shallow depths.

#### Stage 2 (200–140 cm)

The median size ranged from 28.68 to 18.39  $\mu\text{m}$ , with an average median size of 22.83  $\mu\text{m}$ , exclusively comprising silt particles. The sorting ranged from 1.716 to 2.045  $\phi$ , and the skewness ranged from 0.278 to 0.422  $\phi$ , indicating predominantly highly positive skewness with some positive skewness observed. The kurtosis values ranged from 1.051 to 1.270, with the majority of samples exhibiting a peaked distribution and only a few displaying a moderately peaked state. The sediments during this stage exhibited a relatively homogeneous nature, with the smallest median size observed throughout the entire section, indicating the presence of finer sediment particles. In conjunction with the pollen record, it can be inferred that the precipitation associated with the summer monsoon increased, and weathering intensified during this period, indicating a relatively warm and humid stage. During this stage, the ancient lakes and swamps witnessed an augmentation in water volume and a deepening of water levels.

#### Stage 3 (140–100 cm)

The median size ranged from 44.87 to 21.79  $\mu\text{m}$ , with an average median size of 27.59  $\mu\text{m}$ , predominantly comprising coarse silt. The sorting ranged from 1.814 to 1.942  $\phi$ , while the skewness varied between 0.346 and 0.485  $\phi$ , indicating a significantly positive skewness. The kurtosis values ranged from 1.093 to 1.188, indicating a predominantly peaked distribution in most samples, while only one sample exhibited a moderately peaked state. This stage is characterized by the presence of the coarsest sediments, largest median size, and highest sand content. It signifies a period characterized by decreased precipitation and relatively low temperatures across the region. During this stage, the water volume of the ancient lakes and swamps gradually diminished, leading to a contraction in the water area and a shallowing of the water level.

## DISCUSSION

### Regional geomorphic features and evolution

Lu et al. (2022a) suggested that the Shuangji River basin, which encompasses the Huangshui River, can be divided into two distinct geomorphological systems: the river valley and the red clay hills. The red clay hills represent the remnants of the Neogene

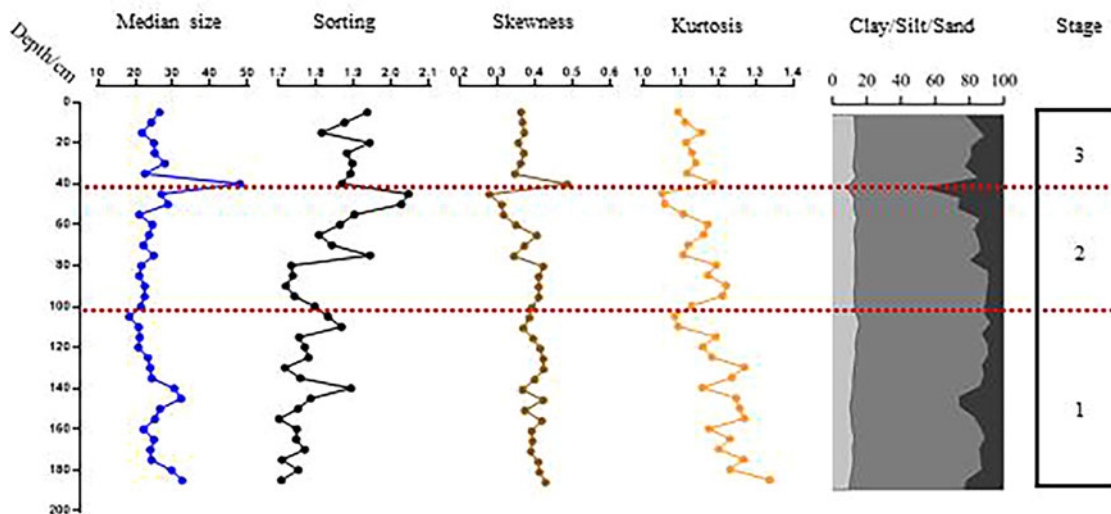


Figure 6. Grain-size analysis of the MD section.



piedmont alluvial fan, which constitutes the foundation of the regional landform. The river valley was formed through significant river downcutting during the Early and Middle Pleistocene (Lu et al., 2019, 2022a). The incision processes have significantly dissected the Neogene piedmont alluvial fan, resulting in the development of a wide and deep valley on its surface. Since then, the river has been confined to the valley and has continuously modified its geomorphic features through incision, silting, and diversion.

The Huangshui River, as a representative minor tributary, exhibits the general geomorphic characteristics observed throughout the Shuangji River basin (Fig. 7). The region can also be divided into two geomorphological systems, namely the red clay hills and the river valley. As the highest geomorphic unit in the region, the red clay hills are distinguished by the Neogene red clay and gravel layers at the base. Based on field investigation and dating results, it has been determined that there are three terraces of different grades within the river valley. The T3 terrace is a strath terrace that formed during the Early Holocene period. Its main sediment is loess, which contains some lenses of lacustrine facies deposits or layers of alluvial sand and gravel. This higher terrace, widely distributed in the region, represents a flat and expansive geomorphic unit. The T2 and T1 terraces are both characterized as fill terraces, which were formed during the end of the Middle Holocene and late historical periods, respectively. These narrow terraces are distributed along the river courses and branching gullies and are primarily composed of sands and gravels.

Specifically, the WJL section, MD section, and ZJW section correspond to the red clay hills, the T3 terrace, and the T2 terrace,

respectively. The dating results for the MD section indicate that ancient lakes and swamps developed on the T3 terrace during the Late Pleistocene to Early Holocene. With the river downcutting, the lakes and swamps gradually drained, and T3 formed around 8 ka. Subsequently, regional rivers experienced prolonged aggradation, leading to the continued rise of the riverbed. However, the floodwater never reached the top of the red clay hills and the T3 terrace during this process. After 4.0 ka, the river underwent another phase of downcutting, gradually forming the narrow T2 terrace. During the late historical period, the river experienced further aggradation and cutting, resulting in the formation of the narrower T1 terrace.

### Regional landscape characteristics reflected by pollen analysis

The pollen record from the MD section provides insights into the regional landscape characteristics at different times. During 10.5–10.0 ka, the dominant vegetation in the region consisted of terrestrial herbaceous plants, with a small presence of ferns and algae. This pollen assemblage further confirms the existence of ancient lakes and swamps in the region during this period, as the presence of hydrogenic herbaceous plants indicates favorable conditions for their growth. Trees and shrubs were sparsely distributed around the lakes, while the occurrence of hydrogenic herbs, algae, and ferns suggests a moderate level of humidity in the area.

During 10.0–9.2 ka, there was a significant increase in the abundance of aquatic herbs, trees, and shrubs, accompanied by a slight rise in algae and ferns. These findings indicate that the area of the ancient lakes and swamps expanded continuously

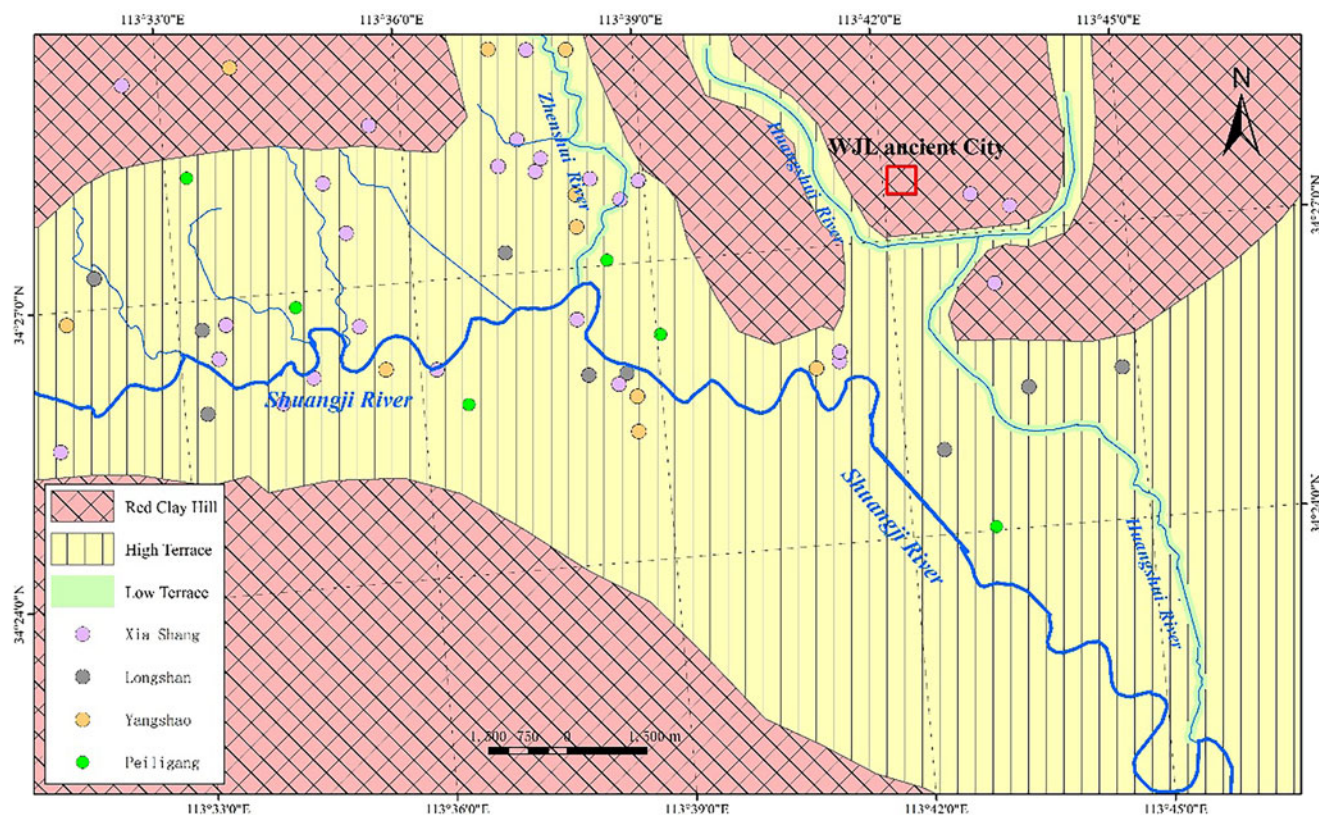


**Figure 7.** The geomorphological map shows that all prehistoric settlements within the Huangshui River basin are situated on the higher geomorphic units due to their landscape stability.

during this period, providing an improved habitat for moisture-loving plants.

From 9.2 to 8.6 ka, the regional vegetation remained dominated by terrestrial herbs. However, the proportion of trees, shrubs, and aquatic herbs decreased compared to the previous period, suggesting a gradual reduction in the extent of the ancient lakes and swamps. After 8.0 ka, the ancient lakes in the research region completely disappeared.

Based on the vegetation evolution reflected by the pollen analysis, the regional landscape exhibited the characteristics of long-term stability. Terrestrial plants always constituted the dominant vegetation type. After the complete disappearance of ancient lakes around 8.0 ka, large-scale water areas no longer existed on the higher geomorphic units.

### ***Landscape stability supported the sustainable development of ancient culture***

The ancient culture in Central China, represented by the Huangshui River basin, is renowned for its uninterrupted and continuous development over thousands of years. Although there are many factors facilitating the sustainable development of the ancient culture, regional landscape stability played a crucial role in this process.

The Huangshui River basin has widely distributed higher topographic units, such as red clay hills and T3 terraces. However, most prehistoric settlements were located on these higher geomorphic positions. After the disappearance of the ancient lakes and swamps around 8.0 ka, the formation of large-scale areas of water ceased on the red clay hills and T3 terraces. Despite the ongoing rise of the riverbed due to river accretion in the region, floodwaters never reached the top of these geomorphic units, indicating a stable landscape. This stability of the landscape supported the long-term and sustainable development of the regional ancient culture.

### ***Regional environmental evolution and the rise of the WJL ancient city***

The WJL city site was situated on top of a red clay hill. This ancient city was established during the Erlitou culture and Erligang culture periods, approximately 4.0 ka. In the Huangshui River basin, the T3 and T2 terraces formed around 8.0 ka and 4.0 ka, respectively. Consequently, there has been a significant elevation difference between the top of the red clay hill, T3 terrace, and the water surface of the river since the formation of the T3 terrace. This height difference effectively protected the platform from the risk of river flooding.

As the rivers continued to incise and the T2 terrace formed after 4.0 ka, this height difference became even more pronounced. The hydrologic environment on the platform, predominantly consisting of aeolian deposits, gradually stabilized during this process. Under these safer natural conditions, the WJL ancient city was constructed, representing a significant milestone in the rise of the Xia and Shang dynasties within the region.

## **CONCLUSIONS**

The region includes two distinct geomorphic systems, namely the red clay hills and the river valley. The red clay hills, formed in the Neogene, represent remnants of the Songshan piedmont alluvial fan that was eroded by rivers. There are three grades of terraces

within the river valley. T3 is a strath terrace and formed around 8.0 ka. Both T2 and T1 are fill terraces, which were developed around 4.0 ka and during the historical period, respectively.

The sedimentary features and pollen analysis indicate the existence of an ancient lake-swamp on the platform during 11.0–9.0 ka. This waterbody gradually shrank during 9.0–8.0 ka, and ultimately disappeared after 8.0 ka.

After the disappearance of the ancient lakes around 8.0 ka, the development of large-scale areas of water ceased on the higher geomorphic units such as the red clay hills and T3 terrace. River floods also cannot reach the top of these high geomorphic units, where numerous prehistoric settlements are located. The stability of the regional landscape has supported the long-term and sustainable development of the ancient culture.

The Xia–Shang cities of the WJL site are situated on a red clay hill. The significant height difference has consistently protected the top of the platform from the threat of river flooding. This excellent natural condition has facilitated the construction and development of the WJL ancient cities, which indicated the rise of the Xia–Shang dynasties in the region.

**Acknowledgments.** The authors would like to express their sincere gratitude to the anonymous reviewers for their valuable comments and constructive suggestions, which have significantly contributed to the improvement of this manuscript. The study is funded by the Chinese Academy of Social Sciences of Social Research Project (Grant No. 2024QNZX029), the Chinese Academy of Social Sciences Youth Fund (Grant No. 2024QQJH063), the Innovation Program at the Institutes of the Chinese Academy of Social Sciences Grant No. 2024KGYJ016, the National Key Research and Development Program of China (Grant No. 2020YFC1521605), the National Natural Science Foundation of China (Grant No. 41971016 and 41671014), the National Key R&D Program of China (Grant No. 2022YFF0903500), the National Social Science Foundation of China (Grant No. 19ZDA227), the Science and Technology Project of Henan Province (Grant No. 232102320165), the Joint Fund of Henan Province Science and Technology R&D Program (Grant No. 225200810048), the Study of Environment Archaeology in Zhengzhou, the Specially-appointed Researcher of Henan (Grant No. 230501009, 220501003), the basic scientific research of Henan Academy of Sciences (Grant Nos. 230601063 and 230601065), and the Innovation Team Project of Henan Academy of Sciences (Grant No. 20230103).

## **References**

- Chen, P., Lu, P., Yang, S., Storozum, M., Yang, R., Tian, Y., Wang, H., *et al.*, 2021. The impact of ancient landscape changes on the city arrangement of the early Shang Dynasty Capital Zhengzhou, Central China. *Frontiers in Earth Science* 9, 656193. <https://doi.org/10.3389/feart.2021.656193>.
- Chen, X.L., You, Y., Wu, Q., 2018. The process of agricultural complication in Xia-Shang Period in Wangjinglou Site of Xinzheng from livestock rearing mode. *Cultural Relics in Southern China* 2, 200–207.
- Dong, G.H., Xia, Z.K., Liu, D.C., Wu, Q.L., 2006. Environmental change and its impact on human activities in Middle Holocene at Mengjin, Henan Province. *Acta Scientiarum Naturalium Universitatis Pekinensis* 2, 238–243.
- Durcan, J.A., King, G.E., Duller, G.A., 2015. DRAC: dose rate and age calculator for trapped charge dating. *Quaternary Geochronology* 28, 54–61.
- Feng, Y.H., 2019. The Evolution of Xinzheng Wangjinglou Xia and Shang Dynasty City Settlement and Social Changes. PhD thesis, Henan University, China.
- Folk, R.L., Ward, W.C., 1957. Brazos river bar: a study in the significance of grain size parameters. *Journal of Sedimentary Petrology* 27, 3–26.
- García, A., Zarate, M., Paez, M.M., 1999. The Pleistocene/Holocene transition and human occupation in the central Andes of Argentina: Agua de lacueva locality. *Quaternary International* 53/54, 43–52.

- Gu, W.F., Wang, Y., Sun, K., Jiao, J.T., Wu, Q., 2012. Excavation report of the Eastern Gate No.1 of the city site of Erligang Culture in Wangjinglou, Xinzheng, Henan. *Cultural Relics* 9, 4–15. <https://doi.org/10.13619/j.cnki.cn11-1532/k.2012.09.001>.
- He, N., 2018. Taosi: an archaeological example of urbanization as a political center in prehistoric China. *Archaeological Research in Asia* 14, 20–32.
- Kidder, T.R., Adelsberger, K.A., Arco, L.J., Schilling, T.M., 2005. Basin-scale reconstruction of the geological context of human settlement: an example from the lower Mississippi Valley, USA. *Quaternary Science Reviews* 27, 1255–1270.
- Lai, Z., Ou, X., 2013. Basic procedures of optically stimulated luminescence (OSL) dating. *Progress in Geography* 32, 683–693.
- Liao, Y.N., Lu, P., Mo, D.W., Wang, H., Storozum, M.J., Chen, P.P., Xu, J.J., 2019. Landforms influence the development of ancient agriculture in the Songshan area, Central China. *Quaternary International* 521, 85–89.
- Liu, B., Wang, N.Y., Chen, M.H., Wu, X.H., Mo, D.W., Liu, J.G., Xu, S.J., Zhuang, Y.J., 2017. Earliest hydraulic enterprise in China, 5,100 years ago. *Proceedings of the National Academy of Sciences* 114, 13637–13642.
- Liu, F.G., Zhang, Y.L., Feng, Z.D., Hou, G.L., Zhou, Q., Zhang, H., 2010. The impacts of climate change on the Neolithic cultures of Gansu-Qinghai region during the late Holocene Megathermal. *Journal of Geographical Sciences* 20, 417–430.
- Lü, J.Q., Mo, D.W., Zhuang, Y.J., Jiang, J.Q., Liao, Y.N., Lu, P., Ren, X.L., Feng, J., 2019. Holocene geomorphic evolution and settlement distribution patterns in the mid-lower Fen River basins, China. *Quaternary International* 521, 16–24.
- Lu, P., Tian, Y., Chen, P.P., Mo, D.W., 2016. Spatial and temporal modes of prehistoric settlement distribution around Songshan Mountain. [In Chinese with English abstract.] *Acta Geographica Sinica* 71, 1629–1639.
- Lu, P., Tian, Y., Yang, R.X., 2012. The study of size-grade of settlements around the Songshan mountain in 9000-3000 aBP based on SOFM networks. *Acta Geographica Sinica* 67, 1375–1382.
- Lu, P., Wang, H., Chen, P.P., Storozum, M.J., Xu, J.J., Tian, Y., Mo, D.W., Wang, S.Z., He, Y., Yan, L.J., 2019. The impact of Holocene alluvial landscape evolution on an ancient settlement in the southeastern piedmont of Songshan Mountain, Central China: a study from the Shiyuan site. *Catena* 183, 104232. <https://doi.org/10.1016/j.catena.2019.104232>.
- Lu, P., Xu, J.J., Wang, X., Hu, Y.Y., Wang, H., 2022b. Research progress and prospect of Holocene vegetation succession in the Songshan Region. *Scientia Geographica Sinica*, 42, 730–738.
- Lu, P., Xu, J.J., Zhuang, Y.J., Chen, P.P., Wang, H., Tian, Y., Mo, D.W., et al., 2022a. Prolonged landscape stability sustained the continuous development of ancient civilizations in the Shuangji River valley of China's Central Plains. *Geomorphology* 413, 108359. <https://doi.org/10.1016/j.geomorph.2022.108359>.
- Macklin, M.G., Lewin, J., 2015. The rivers of civilization. *Quaternary Science Reviews* 114, 228–244.
- Murray, A.S., Wintle, A.G., 2003. The single aliquot regenerative dose protocol: potential for improvements in reliability. *Radiation Measurements* 37, 377–381.
- National Cultural Heritage Administration, 1991. *Atlas of Chinese Cultural Relics Henan Volume*. China Map Publishing House, Beijing.
- National Cultural Heritage Administration, 1999. *Atlas of Chinese Cultural Relics Shaanxi Volume*. China Map Publishing House, Beijing.
- National Cultural Heritage Administration, 2003. *Atlas of Chinese Cultural Relics Hubei Volume*. China Map Publishing House, Beijing.
- Ren, X.L., Xu, J.J., Wang, H., Storozum, M., Lu, P., Mo, D.W., Li, T.Y., Xiong, J.G., Kidder, T.R., 2021. Holocene fluctuations in vegetation and human population demonstrate social resilience in the prehistory of the Central Plains of China. *Environmental Research Letters* 16, 055030. <https://doi.org/10.1088/1748-9326/abdfoa>.
- Shimada, I., Schaaf, C.B., Thompson, L.G., Mosley-Thompson, E., 1991. Cultural impacts of severe droughts in the prehistoric Andes: application of a 1,500-year ice core precipitation record. *World Archaeology* 22, 247–270.
- Sun, Z.Y., Shao, J., Liu, L., Cui, J.X., Bonomo, M.F., Guo, Q.H., Wu, X.H., Wang, J.J., 2018. The first Neolithic urban center on China's north Loess Plateau: the rise and fall of Shimao. *Archaeological Research in Asia* 14, 33–45.
- Tinner, W., Conedera, M., Gobet, E., Hubschmid, P., Wehrli, M., Ammann, B., 2000. A palaeoecological attempt to classify fire sensitivity of trees in the southern Alps. *Holocene* 5, 565–574.
- Wang, F.X., Qian, N.F., Zhang, Y.L., Xu, Q.H., 1995. *Pollen Morphology of Chinese Plants*. Science Press, Beijing.
- Wang, S.Y., Wang, Y.Z., Wang, Z.Y., 1989. Characteristics of the vegetation in Henan Province *Acta Agriculturae Universitatis Henanensis* 23, 386–392.
- Wang, Z.H., Ryves, D.B., Lei, S., Nian, X.M., Lv, Y., Tang, L., Wang, L., Wang, J.H., Chen, J., 2018. Middle Holocene marine flooding and human response in the south Yangtze coastal plain, East China. *Quaternary Science Reviews* 187, 80–93.
- Wilson, K.M., McCool, W.C., Brewer, S.C., Zamora-Wilson, N., Schryver, P.J., Lamson, R.L.F., Huggard, A.M., Coltrain, J.B., Contreras, D.A., Coddling, B.F., 2022. Climate and demography drive 7000 years of dietary change in the Central Andes. *Scientific Reports* 12, 2026. <https://doi.org/10.1038/s41598-022-05774-y>.
- Wu, Q., 2022. Study on animal bones excavated from Erligang Cultural of the Wangjinglou Site. *Huaxia Archaeology* 3, 63–69.
- Wu, Q., Wei, Q.L., Bo, T.R., 2011. A report on the preliminary investigation and excavation of Erligang Culture at Wangjinglou. *Journal of National Museum of Chinese History* 10, 19–28.
- Xu, H., Chen, G.L., Zhao, H.T., 2004. A preliminary investigation of the settlement pattern at Erlitou Site. *Archaeology* 11, 23–31.
- Xu, J.J., Mo, D.W., Wang, H., Zhou, K.S., 2015. Preliminary research of environment archaeology in Zhengshui river, Xinmi city, Henan. *Quaternary Science* 33, 954–964.
- Zhang, G.S., 2012. The Wangjinglou Xia Dynasty city site and Kunwu area. *Journal of Soochow University* 33, 7. <https://doi.org/10.19563/j.cnki.szds.2012.01.031>.
- Zhang, J., Mo, D., Xia, Z., Qi, W., Wang, H., Wang, X., Zhou, L., 2009. Optical dating of sediments from China and its implication for depositional processes. *Quaternary Science*, 29, 23–33.
- Zhang, X.H., Yang, S.G., Lu, P., Li, Y.P., Chen, P.P., Xia, Z.K., 2022. Holocene landscape evolution and its interaction with human activities in the southern piedmont of Taihang Mountain, Central China. *Frontiers in Plant Science* 13, 980840. <http://doi.org/10.3389/fpls.2022.980840>.
- Zhou, K.S., Zhang, S.L., Zhang, Z.Y., Yang, R.X., Cai, Q.F., Song, G.D., Song, Y.Q., et al., 2005. Mountain Song culture circle. *Cultural Relics of Central China* 1, 12–20.